

Enhanced Degradation Resistance of Quantum Dot Lasers to Radiation Damage

P.G. Piva^{a)}, R.D. Goldberg, I.V. Mitchell
Department of Physics
University of Western Ontario, London, Ontario, N6A 3K7, Canada

D. Labrie
Department of Physics
Dalhousie University
Halifax, Nova Scotia, B3H 3J5, Canada

R. Leon
Jet Propulsion Laboratory,
California Institute of Technology,
Pasadena, California, 91109, U.S.A.

and,

S. Charbonneau^{b)}, Z.R. Wasilewski, S. Fafard
Institute for Microstructural Sciences
National Research Council Canada
Ottawa, Ontario, K1A 0R6, Canada

ABSTRACT

We compare the degradation of InAs/GaAs quantum well (QW) and quantum dot (QD) laser diodes following irradiation by high energy (8.56 MeV) phosphorous ions. Over a fluence range of 10^8 to 10^{11} ions/cm², the degradation of the low temperature QD photoluminescence and electroluminescence emission is greatly suppressed relative to that of QW based devices (x100 and x1000, respectively at the highest dose studied). Irradiated QD laser diodes demonstrated lasing action over the entire range of fluences, and 2 orders of

magnitude beyond the maximum dose sustainable by QW devices. The improved damage response of QD based structures results from efficient collection and localisation of electrons and holes by QDs in the active region, which limit carrier transfer to nonradiative centres. This work suggests the suitability of QD device architectures for use in radiation environments, and in high power applications wherever nonradiative processes promote the degradation or failure of traditional QW devices.

Self-assembled semiconductor quantum dots (QD) formed during the initial stages of Stranski-Krastanow growth are under investigation as an alternate platform for traditional quantum-well (QW) based optoelectronic components. The low density of states, and sharply defined eigenenergy levels in these zero-dimensional structures allow the fabrication of devices with improved and often novel characteristics.¹⁻³ Of relevance to the present work are observations concerning the efficient transfer of carriers to the QDs in the midst of nonradiative centres. As carriers relaxing to bound states within QDs will generally remain trapped until recombining radiatively, QDs present in areal or volumetric concentrations in excess of those of nonradiative centres will be able to effectively compete against nonradiative processes occurring at these sites. This capability of QD structures allowed the deposition of optically active InAs QDs on silicon⁴, and led to the observation of enhanced photoluminescence (PL) degradation resistance to Argon plasma damage,⁵ and to displacement damage generated by ion implantation in InGaAs/GaAs^{6,7} and InAs/GaAs⁸ QD structures.

We report on the differential damage response of *p-i-n* InAs/GaAs/AlGaAs QD and QW laser diodes following irradiation by high energy phosphorous ions (8.56 MeV). Over a fluence range of 10^8 to 10^{11} ions/cm², the low temperature PL and electroluminescence (EL) intensities of QW based structures exhibit a decrease of 2 and 3 orders of magnitude, respectively, in excess of that observed in QD structures resulting from the enhanced relative in-plane carrier

mobility in QW epilayers. Laser diodes fabricated from the irradiated QD material demonstrated lasing action over the entire range of fluences studied, and 2 orders of magnitude beyond the maximum dose sustainable by QW devices.

The QW and QD *p-i-n* samples were grown by MBE as described elsewhere.⁹ The device structures consisted of a thick ($\sim 2 \mu\text{m}$) n^+ - $\text{Al}_{0.7}\text{Ga}_{0.3}\text{As}$ contact layer followed by a graded (134 nm) $\text{Al}_{0.7 \rightarrow 0.33}\text{Ga}_{0.3 \rightarrow 0.67}\text{As}$ bottom cladding layer with lower doping followed by the active region, and then by a symmetric p-doped graded $\text{Al}_{0.33 \rightarrow 0.7}\text{Ga}_{0.67 \rightarrow 0.30}\text{As}$ cladding layer and contact layer (1.47 μm) capped with 300 nm of p^+ -GaAs. The undoped active region of the QW (QD) structure was grown between two 15 nm GaAs layers, and consisted of 7 repeats of 1.8 (2.5) monolayers (ML) of InAs separated by 10 nm GaAs barriers. For the QD sample, an InAs coverage of 2.5 ML was selected, resulting in Stranski-Krastanow island formation with a mean dot diameter of ~ 20 nm and an areal density of $\sim 10^{10} \text{ cm}^{-2}$. An indium-flush⁹ was performed midway through the deposition of each GaAs spacer layer to improve the uniformity of the QD size. A spacer layer thickness of 10 nm allowed strain propagation through the GaAs layers, inducing vertical self alignment of the QDs during growth.¹⁰

The ion irradiations were carried out using the 1.7 MV Tandem accelerator facility located at the University of Western Ontario. Samples were implanted at room temperature using 8.56 MeV P^{4+} ions and oriented 7° off-normal to minimise the effects of ion channelling. The mean ion range calculated by TRIM-

97^{11} was $3.57 \mu\text{m}$ placing the P ions well into the AlGaAs cladding nearest the substrate. Samples were unmasked, and implanted with fluences ranging from 10^8 to 10^{11} ions/cm² using a flux of 0.02 nA/cm^2 . As the InAs QW and QD structures were nominally identical (differing only by 7×0.7 ML of InAs in the active region) the large scale damage distributions created in these samples are indistinguishable, while the effect of the additional InAs coverage in the QD samples will tend to increase the displacement damage accumulated by these layers relative to the QW samples.

Continuous-wave PL measurements monitored the extent of the damage created by the P implants. The measurements were performed at 4.2 K using weak HeNe excitation (10 W/cm^2) at a wavelength of 632.8 nm. The spectra were collected using a BOMEM FTIR fitted with an InGaAs detector. The PL spectra acquired from unirradiated control samples, and the four implanted QW and QD samples appear in figures 1 (a) and (b), respectively. The peak emission wavelength for the QWs (QDs) in the QW (QD) samples was 867 nm ($1.01 \mu\text{m}$). Also apparent in the QW samples is a broad luminescent feature centred at 946 nm corresponding to PL emission from a sparse distribution of QDs formed on the QWs during growth. The areal density of this unintentional QD population is $\sim 10^8 \text{ cm}^{-2}$.¹² The slight redshift in the as-grown QD peak emission wavelength ($1.02 \mu\text{m}$) relative to those of the irradiated QD samples in figure 1 (b) results from differences in deposition rates across the growth wafer and appears as this sample was cleaved from a different location relative to the

irradiated samples.

While the QW PL intensity at 867 nm is all but quenched at a dose of 10^{11} ions/cm², the QD PL emission presented in figure 1 (b) remains evident over the entire range of fluences. Figure 1 (c) shows the integrated PL intensity ratios taken between QW and QD samples (solid circles) mounted side by side in the cryostat for a given dose with errors due to sample misalignment not exceeding the 20% indicated. In this curve, the luminescence intensity of the QWs is seen to decrease by a factor of 100 more than the corresponding changes induced in the QDs (a conservative estimate, as the luminescence in the vicinity of 867 nm at a dose of 10^{11} cm⁻² is dominated by the luminescence feature centred at 858 nm and more properly attributed to the substrate¹³). The solid square trace in figure 1 (c) corresponds to the QW PL intensity ratio taken with respect to the unintentional QD emission (at 946 nm) in each of the QW samples. This ratio is not subject to alignment error, and serves as a complementary means of investigating the differential response of the QDs and QWs to the displacement damage. While both curves are in general agreement, the amplitude of the PL attenuation (x32) for the solid square curve is smaller than the factor of 100 determined above. This, however, may be expected as nonradiative events occurring in the QWs will also decrease the number of carriers available for recombination in the unintentional QDs. These results compare favourably with observations by others⁴⁻⁸ and are understood in terms of the efficient relaxation, and localisation of carriers by QDs, which limit subsequent transfer to

nonradiative centres.

Figures 2 (a) and (b), show the 77K L-I curves from broad area lasers fabricated from the as-grown control, and irradiated QW and QD samples, respectively. Indium contacts were made to the front (top contact ~ 1 mm in diameter) and back surfaces of the 1.5 mm by 4 mm samples without recourse to lithography, and annealed at a temperature of 200 °C for 90s. The devices were driven with a 0.1% duty cycle (5 μ s pulses at 252 Hz) and the integrated light output levels were measured using a commercial powermeter. The response of the QW devices is shown in figure 2 (a). Only the as-grown, and the 10^8 and 10^9 cm^{-2} irradiated devices could achieve stimulated emission, with increases in threshold current being observed at increasing fluences. The 10^{10} and 10^{11} cm^{-2} devices could not achieve threshold, and significantly, demonstrated integrated spontaneous emission intensity levels 2, and 4 orders of magnitude lower than the as grown sample below threshold. While these trends compare favourably with those exhibited by the QW PL intensities at 4.2K, the larger attenuations (x10) relative to the as-grown QW samples may result from the fact that these measurements were performed at higher temperature (77 K) where increased carrier diffusion lengths should allow a greater portion of electrons and holes to encounter nonradiative centres prior to recombining. Conversely, all QD devices achieved threshold in figure 2 (b), with only the 10^{11} cm^{-2} sample demonstrating a significant increase in threshold current, and decrease (x4) in spontaneous emission intensity below threshold with respect to as-grown sample (and in

qualitative agreement with observed variations in absolute PL intensity levels in figure 1 (b)). The lack of any significant enhancement in the EL attenuation relative to 4.2K PL data is a further indication of the highly localised nature of the carriers in the QDs.

The overall trends established by the QW samples, and the as-grown, 10^8 , and 10^{11} cm^{-2} QD samples indicate increasing threshold currents at higher irradiation fluences. This is consistent with the increasing displacement damage levels and corresponding nonradiative losses occurring in these devices.¹⁴ While all QD devices lased with threshold current densities below 100 A/cm^2 , it is unclear in all instances whether the changes observed in threshold current translate to similar changes in threshold current density (particularly given the counterintuitive decreases in threshold current in the QD devices following the 10^9 and 10^{10} cm^{-2} irradiations). As the upper indium p-contacts were simply annealed onto the topmost p-GaAs layer, without patterning, variations in the effective contact area (x2) beneath p-side indium contacts might be expected, and could easily account for the observed scatter in these lower dose samples. Additionally, the differential efficiencies of both the lasing QW and QD devices actually increase by a factor of two or three above the as-grown levels (1.5%, and 2.5% for the QW and QD devices, respectively) after having received implant doses of 10^8 and 10^9 P ions/ cm^2 (and again at 10^{11} cm^{-2} for the QD samples). The absence of any clear trend indicating decreasing differential efficiencies at higher doses for both the QW and QD devices (in spite of the progressive decreases observed in

both PL and spontaneous EL intensities with dose) runs counter to expectation. It seems equally probable that this effect results from difficulties with the upper contact. As our devices lack proper lateral confinement of the carrier injection region, or of the optical mode as would be afforded by ridge-waveguide lasers, the observed scatter in efficiencies (or post threshold L-I slopes) may easily result from spatial inhomogeneities in current flow across the gain-guided optical cavities in our devices resulting from variations in the contact resistivity beneath indium contact regions (and expected to vary from one device to the next). Further experiments involving lithographically defined ridge-waveguide lasers of differing geometries would be required to unambiguously ascertain the dependence of the many important device parameters on the implant damage (i.e. threshold current densities, internal quantum efficiencies, loss coefficients, etc.) It is important to emphasise, however, that while these fabrication issues may lead to some degree of scatter in the operational device parameters, they do not affect the more fundamental nature of the EL observations below threshold where the emission intensities vary in proportion to the injection current and the levels of nonradiative recombination occurring in these structures. Given the importance of efficient radiative carrier recombination in establishing conditions for optical gain, the failure of the 10^{10} and 10^{11} cm^{-2} irradiated QW devices to achieve threshold is to be understood in terms of the x100 and x10 000 decreases in the EL intensity relative to the as-grown control sample and not as resulting from those lesser effects described above in relation to the nature of the device fabrication.

In summary, we have determined that active QD optoelectronic devices such as laser diodes can sustain significantly greater irradiation fluences ($\times 100$) than comparable QW based structures prior to the onset of failure. This differential response of p-i-n based QW and QD devices is also evident in the induced changes to the spontaneous emission levels below threshold, and are shown to be in qualitative agreement with trends established by PL measurements. The increased functionality of these devices is understood in terms of the reduced in-plane carrier mobility in the QD active region, and the corresponding suppression of charge transfer to nonradiative centres. This work suggests the suitability of QD device architectures for use in radiation environments, and in high power applications wherever nonradiative processes are known to result in the degradation or failure of traditional QW devices.

This work was partially supported by NSERC.

REFERENCES

- a) Visiting student with the Institute for Microstructural Sciences at the National Research Council of Canada
Electronic mail: paul.piva@nrc.ca
- b) Also an Adjunct Professor with the Dept. of Physics and Astronomy, University of Western Ontario.
- ¹ S. Fafard, K. Hinzer, S. Raymond, M. Dion, J. McCaffrey, Y. Feng, S. Charbonneau, *Science* **274** 1350 (1996)
- ² N.N. Ledentsov, *Semiconductors* **33** 946 (1999) and references therein.
- ³ S.J. Xu, S. J. Chua, T. Mei, X.C. Wang, X.H. Zhang, G. Karunasiri, W.J. Fan, C.H. Wang, J. Jiang, S. Wang, X.G. Xie, *Appl. Phys. Lett.* **73** 3153 (1998)
- ⁴ J.M. Gerard, O. Cabrol, B. Sermage, *Appl. Phys. Lett.* **68** 3123 (1996)
- ⁵ W.V. Schoenfeld, C.-H. Chen, P.M. Petroff, E.L. Hu, *Appl. Phys. Lett.* **73** 2935 (1998)
- ⁶ P.G. Piva, R. Leon, S. Fafard, S. Charbonneau, R.D. Goldberg, I.V. Mitchell, unpublished, 1997.
- ⁷ R. Leon, G.M. Swift, B. Magness, W.A. Taylor, Y.S. Tang, K.L. Wang, P. Dowd, Y.H. Zhang, *Appl. Phys. Lett.* **76** 2074 (2000)
- ⁸ P.J. Wellmann, W.V. Schoenfeld, J.M. Garcia, P.M. Petroff, *J. Electr. Mat.* **27** 1030 (1998)

- ⁹ S. Fafard, Z.R. Wasilewski, C. Ni. Allen, K. Hinzer, J.P. McCaffrey, Y. Feng, Appl. Phys. Lett. **75** 986 (1999)
- ¹⁰ L. Goldstein, F. Glas, J.Y. Marzin, M.N. Charasse, G. LeRoux, Appl. Phys. Lett. **47** 1099 (1985)
- ¹¹ J.F. Ziegler, J.P. Biersack, U. Littmark, *The Stopping and Ion Range of Ions in Matter* (Pergamon, New York, 1985)
- ¹² S. Fafard, Z.R. Wasilewski, M. Spanner, Appl. Phys. Lett. **75** 1866 (1999)
- ¹³ the PL feature centred at 858 nm was greatly enhanced relative to the QW and QD features when exciting at a wavelength of 800 nm, and was absent from the EL spectra
- ¹⁴ C.E. Barnes, D. Heflinger, R. Reel, SPIE Conf. Proc. **1314** 168 (1990)

FIGURE CAPTIONS

Fig. 1: Low temperature (4.2 K) PL spectra for as-grown and irradiated (a) QW, and (b) QD device structures. Solid, dashed, dotted, dash-dotted, and dashed double-dotted lines correspond to as-grown, and 10^8 , 10^9 , 10^{10} , and 10^{11} cm^{-2} irradiated samples, respectively. The PL feature centred at ~ 835 nm and present in figures 1 (a) and (b) is GaAs related. Figure 1(c) shows the ratio of the integrated PL intensity between the QW and QD samples (solid circles), and the QW and unintentional QDs (solid squares) as a function of irradiation dose.

Fig. 2: Light output vs. pump current for (a) QW, and (b) QD broad area laser diodes measured at 77 K. Solid, dashed, dotted, dash-dotted, and dashed double-dotted lines correspond to as-grown, and 10^8 , 10^9 , 10^{10} , and 10^{11} cm^{-2} irradiated samples, respectively.

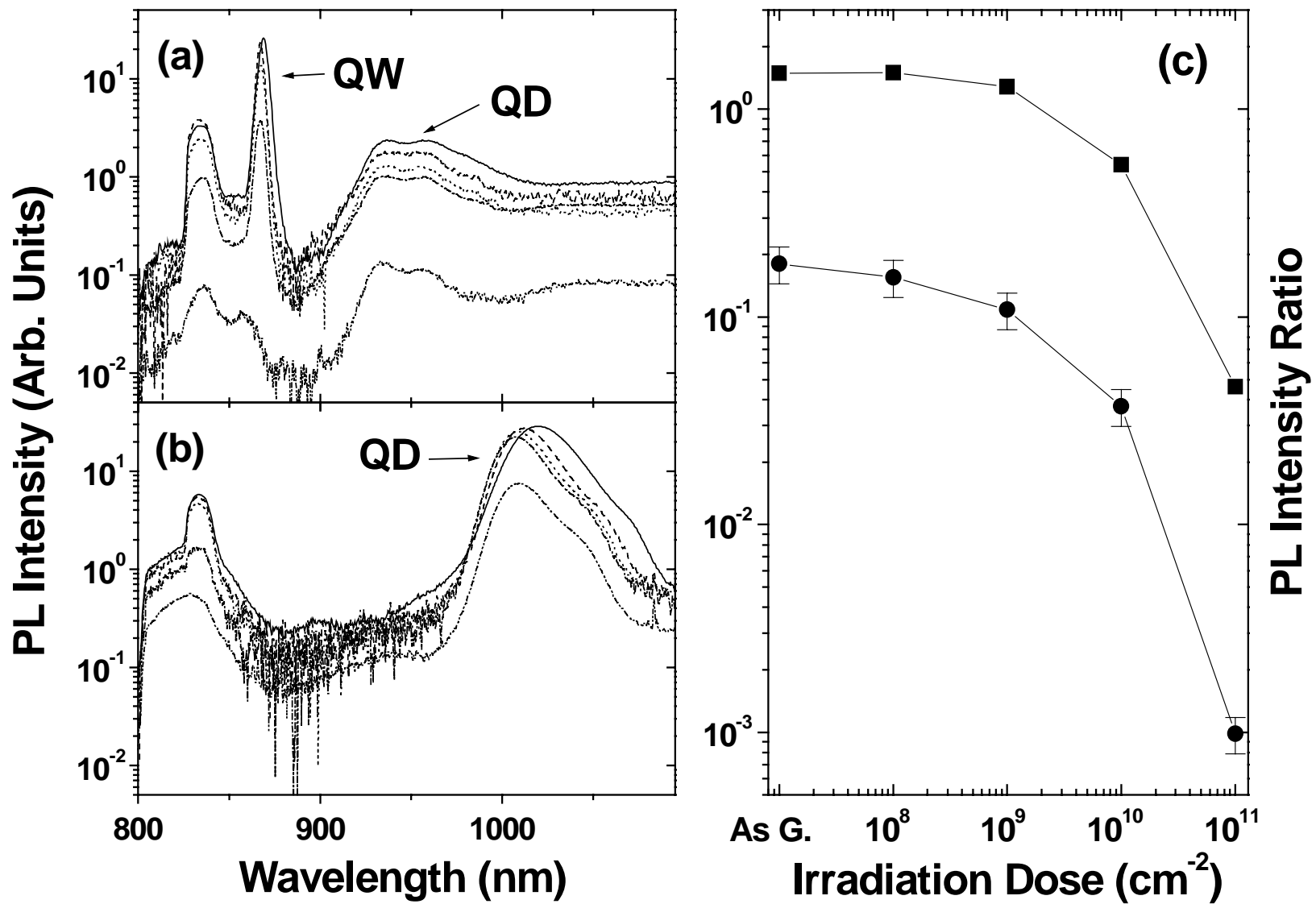


Fig. 1: Piva et al.

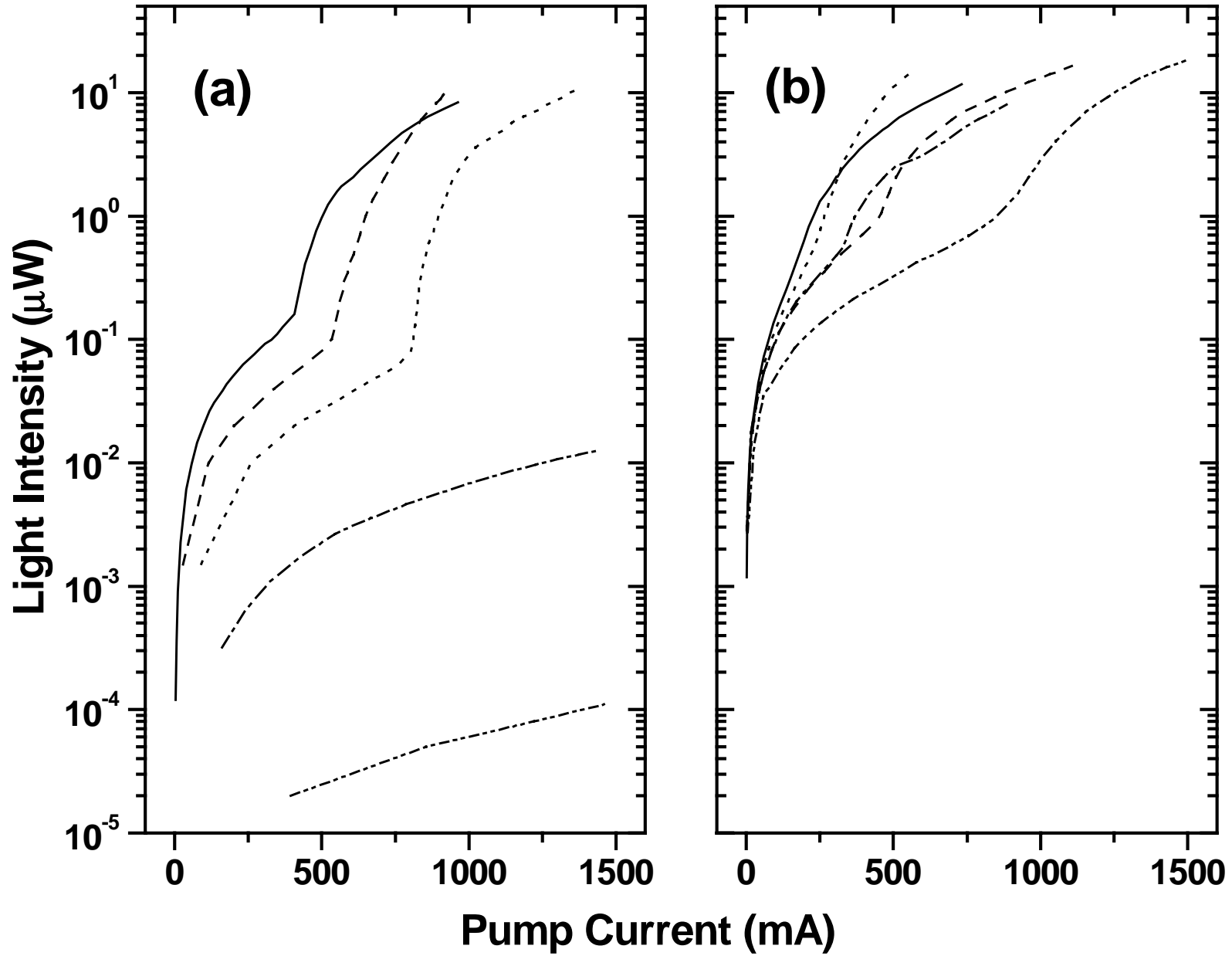


Fig 2: Piva et al.